

Dynamics of the maximum marginal likelihood hyper-parameter estimation in image restoration : gradient descent vs. EM algorithm

Jun-ichi Inoue

*Complex Systems Engineering, Graduate School of Engineering,
Hokkaido University, N13-W8, Kita-ku, Sapporo 060-8628, Japan*

Kazuyuki Tanaka

*Department of Computer and Mathematical Science, Graduate School of Information Science,
Tohoku University, Aramaki-aza-aoba 04, Aoba-ku, Sendai 980-8579, Japan*

(December 2, 2024)

Abstract

Dynamical properties of image restoration and hyper-parameter estimation are investigated by means of statistical mechanics. We introduce an exactly solvable model for image restoration and derive the differential equations with respect to macroscopic quantities. From these equations, we evaluate relaxation processes of the system to its equilibrium state in the sense of the Markov chain Monte Carlo method. Our statistical mechanical approach also enable one to investigate the hyper-parameter estimation by means of maximization of marginal likelihood using gradient decent, or the EM algorithm from dynamical point of view.

PACS numbers : 02.50.-r, 05.20.-y, 05.50.-q

I. INTRODUCTION

As a typical massive system, image restoration based on the Markov random field (MRF) model has been investigated by statistical mechanics of disordered spin systems [1–4]. Among these results, statistical mechanical analysis succeeded in evaluating the measure of successfulness of image restoration and made its hyper-parameter dependence clear [2–4]. However, all of those researches are restricted to the study of the static properties of the algorithm of image restoration. In practical situation for image restoration in the context of Bayesian approach, we usually use the Markov chain Monte Carlo (MCMC) method to obtain the maximum a posteriori (MAP) estimate by simulated annealing [5], or to calculate the expectation over the posterior distribution for the maximum posterior marginal (MPM) estimation [6]. In the recent study by Nishimori and Wong [2], they introduced the infinite range version of the MRF model and calculated the overlap between the original image and restored one, and investigated its hyper-parameter dependence quantitatively. However, they did not mention about the process of the image restoration, that is to say, the process of the MCMC method to obtain the MPM estimate. Although it is worth while to investigate such dynamical processes in image restoration, relatively little progress has been made in the theoretical understanding of them. In addition, it is important to study how we should infer the optimal hyper-parameters before hand. Recently, one of the authors [7] investigated the maximum marginal likelihood (MML) method to estimate the hyper-parameters [8] in the context of so-called mean-field approximations. If we maximize the marginal likelihood by the assistance of the gradient descent, we obtain Boltzmann machine-type learning equations and usually these equations contain the expectations over both the posterior and the prior. In order to carry out those expectations, we usually use the MCMC method besides mean-field approximation. However, it is hard to evaluate the performance of the MML estimation due to difficulties to realize the thermo-dynamically equilibrium state within reliable precision.

For these reasons, we need some analytical and rigorous studies on the hyper-parameter estimation. Obviously, the process of the hyper-parameter estimation described by the learning equations, or the stochastic process of the MCMC method to evaluate the expectations are regarded as dynamics. And as long as we know, no studies have ever tried to investigate those dynamical properties analytically. In this paper, we investigate the dynamical properties of image restoration and hyper-parameter estimation by using statistical mechanical technique.

This paper is organized as follows. In the next section, according to Nishimori and Wong [2], we explain the statistical mechanical formulation of image restoration in the context of the MPM estimation. In Sec. III, we investigate an infinite range version of the MRF model and derive the differential equations with respect to the macroscopic physical quantities from the microscopic Master equation. We discuss the relaxation processes of the image restoration by solving these differential equations. In Sec. IV, the marginal likelihood as a function of the hyper-parameters is calculated by replica method. We also derive the Boltzmann machine-type learning equations by taking the gradient decent of the marginal likelihood. The flow to the solution in the hyper-parameter space is obtained by using the analysis of the learning equations. In the same section, we investigate the performance of EM algorithm [9] which is a widely used to estimate the hyper-parameters from incomplete data sets. It is well known that EM algorithm show faster convergence to the solution at the beginning of the algorithm than the other methods does. However, there is no study to make this property clear by using some analytically solvable model for massive problems. In this section, we compare the performance of the EM algorithm with that of the gradient descent to maximize the marginal likelihood. The final section is devoted to summary.

II. STATISTICAL MECHANICAL FORMULATION FOR IMAGE RESTORATION

In this section, we explain how we treat the image restoration as a problem of disordered spin system. According to Nishimori and Wong [2], we consider black or white image. Then, the original image is denoted by N -dimensional vector $\{\xi\} \equiv (\xi_1, \xi_2, \dots, \xi_N)$ and each pixel takes $\xi_i = \pm 1$. These pixels are located on arbitrary lattice in two dimension. In order to treat image restoration by statistical mechanics of disordered spin systems, we should assume that the original image is given by the following Boltzmann-Gibbs distribution

$$P(\{\xi\}) = \frac{\exp\left(\beta_s \sum_{ij} \xi_i \xi_j\right)}{Z_s}, \quad Z_s = \sum_{\xi} \exp\left(\beta_s \sum_{ij} \xi_i \xi_j\right) \quad (1)$$

where $\sum_{ij}(\dots)$ is carried out for all nearest neighboring pixels. In other word, we use a snapshot of the MCMC simulation for the ferromagnetic Ising model. $T_s (\equiv \beta_s^{-1})$ appearing in the argument of the exponential (1) corresponds to temperature of the spin system and if we set $T_s \rightarrow 0$, we obtain the image of all black or all white. On the other hand, in the limit of $T_s \rightarrow \infty$, we obtain the random noise picture.

The original image $\{\xi\}$ is degraded to a damaged picture $\{\tau\}$ by the following noise channel as a conditional probability

$$P(\{\tau\}|\{\xi\}) = \frac{\exp\left(\beta_\tau \sum_i \tau_i \xi_i\right)}{[2\cosh\beta_\tau]^N} \quad (2)$$

where sum $\sum_i(\dots)$ is carried out for all pixels and we assumed that each pixel is degraded independently. β_τ represents the noise level because the above expression of noise channel is rewritten as $P(-\xi_i|\xi_i) = p = 1 - P(\xi_i|\xi_i)$ with $p = e^{-\beta_\tau}/(e^{\beta_\tau} + e^{-\beta_\tau})$ for all pixels independently. Therefore, this kind of noise is referred to as *Binary Symmetric Channel* (BSC).

The BSC is easily extended to the following *Gaussian Channel* (GC)

$$P(\{\tau\}|\{\xi\}) = \frac{1}{(\sqrt{2\pi\tau})^N} \exp\left(-\frac{\sum_i(\tau_i - \tau_0\xi_i)^2}{2\tau^2}\right) = F(\{\tau\}) \exp\left(\frac{\tau_0}{\tau^2} \sum_i \tau_i \xi_i\right) \quad (3)$$

$$F(\{\tau\}) = \frac{1}{(\sqrt{2\pi\tau})^N} \exp\left(-\frac{\sum_i(\tau_i^2 + \tau_0^2)}{2\tau^2}\right). \quad (4)$$

If we replace $F(\{\tau\})$ appearing in Eq. (3) by

$$F(\{\tau\}) = \frac{1}{(2 \cosh \beta_\tau)^N} \prod_i \{\delta(\tau_i - 1) + \delta(\tau_i + 1)\} \quad (5)$$

and set $\tau_0/\tau^2 = \beta_\tau$, the BSC is recovered.

In the context of both the MAP and the MPM estimations, we should calculate the posterior by means of the Bayesian theorem

$$P(\{\sigma\}|\{\tau\}) = \frac{P(\{\tau\}|\{\sigma\})P(\{\sigma\})}{\sum_\sigma P(\{\tau\}|\{\sigma\})P(\{\sigma\})} = \frac{e^{J \sum_{ij} \sigma_i \sigma_j + h \sum_i \tau_i \sigma_i}}{\sum_\sigma e^{J \sum_{ij} \sigma_i \sigma_j + h \sum_i \tau_i \sigma_i}} \quad (6)$$

where J and h are hyper-parameters and we introduced the models of the prior and the likelihood as

$$P(\{\sigma\}) = \frac{\exp\left(J \sum_{ij} \sigma_i \sigma_j\right)}{Z_{\text{II}}}, \quad P(\{\tau\}|\{\sigma\}) = \frac{\exp\left(h \sum_i \tau_i \sigma_i\right)}{Z_L}. \quad (7)$$

Z_{II} and Z_L are normalization constants given by

$$Z_{\text{II}} = \sum_\sigma \exp\left(J \sum_{ij} \sigma_i \sigma_j\right), \quad Z_L = \sum_\tau \exp\left(h \sum_i \tau_i \sigma_i\right). \quad (8)$$

In the context of the MAP estimation, we choose the estimate of the original image $\{\sigma\}$ as a grand state of the following Hamiltonian (the energy function)

$$\mathcal{H}(\{\sigma\}) = -J \sum_{ij} \sigma_i \sigma_j - h \sum_i \tau_i \sigma_i. \quad (9)$$

In order to obtain the grand state $\{\sigma\}$, we usually use the simulated annealing [10] or the mean field annealing methods [11].

On the other hand, in the context of the MPM estimation, we first calculate the marginal distribution around a single pixel σ_i ;

$$P(\sigma_i|\{\tau\}) = \sum_{\{\sigma\} \neq \sigma_i} P(\{\sigma\}|\{\tau\}) \quad (10)$$

and we choose the sign of the difference between $P(\sigma_i = +1|\{\tau\})$ and $P(\sigma = -1|\{\tau\})$ as an estimate of the i -th pixel $\hat{\xi}_i$ as

$$\begin{aligned}\hat{\xi}_i &= \operatorname{argmax}_{\sigma_i} P(\sigma_i|\{\tau\}) = \operatorname{sgn} \left(\sum_{\sigma_i=\pm 1} P(\sigma_i|\{\tau\}) \right) = \operatorname{sgn} \left(\frac{\sum_{\sigma} \sigma_i P(\{\sigma\}|\{\tau\})}{\sum_{\sigma} P(\{\sigma\}|\{\tau\})} \right) \\ &\equiv \operatorname{sgn} (\langle \sigma_i \rangle_{J,h}).\end{aligned}\quad (11)$$

In this expression, we define $\langle \sigma_i \rangle_{J,h}$ as an average of the pixel σ_i over the posterior (6) and this is written explicitly as

$$\langle \sigma_i \rangle_{J,h} = \frac{\sum_{\sigma} \sigma_i e^{J \sum_{ij} \sigma_i \sigma_j + h \sum_i \tau_i \sigma_i}}{\sum_{\sigma} e^{J \sum_{ij} \sigma_i \sigma_j + h \sum_i \tau_i \sigma_i}}.\quad (12)$$

This corresponds to a local magnetization of the spin system that is described by the Hamiltonian $\mathcal{H}(\{\sigma\})$ at temperature $T = 1$. The spin system $\mathcal{H}(\{\sigma\})$ is referred to as *random field Ising model*. Thus, in order to investigate the properties of the MPM estimation for image restoration, we should study the random field Ising model described by $\mathcal{H}(\{\sigma\})$. Then, we are interested in the following quantity

$$M(J, h) \equiv \sum_{\tau, \xi} P(\{\xi\}) P(\{\tau\}|\{\xi\}) \xi_i \operatorname{sgn}(\langle \sigma_i \rangle_{J,h})\quad (13)$$

which means the averaged overlap between the original image ξ_i and the restored one $\hat{\xi}_i = \operatorname{sgn}(\langle \sigma_i \rangle_{J,h})$. We easily see that we obtain the best restoration of the original image when the overlap M is as close to 1 as possible. For this averaged overlap $M(J, h)$, the next inequality holds [2].

$$M(J, h) \leq M(\beta_s, \beta_\tau)\quad (14)$$

This inequality means that the averaged overlap M takes its maximum at $J = \beta_s$ and $h = \beta_\tau$. However, it is impossible to derive the hyper-parameter dependence of the overlap around its optimal value $M(\beta_s, \beta_\tau)$ from the above inequality. To investigate this dependence, Nishimori and Wong [2] introduced the infinite range version of the MRF model and calculated the overlap as a function of J and h by using statistical mechanics. This infinite range model is rather an artificial model in which every pixel is connected to

the others, however, this model is very useful to discuss the behavior of the macroscopic quantities of the system, like overlap M . Using the replica trick [14] and the saddle point method, we obtain the equations of state;

$$m_0 \equiv \frac{1}{N} \sum_i \xi_i = \tanh(\beta_s m_0) \quad (15)$$

$$m \equiv \frac{1}{N} \sum_i \sigma_i = \frac{\sum_{\xi} e^{\beta_s m_0 \xi}}{2 \cosh(\beta_s m_0)} \int_{-\infty}^{\infty} Dx \tanh(Jm + \tau h x + \tau_0 h \xi) \quad (16)$$

$$M \equiv \frac{1}{N} \sum_i \xi_i \hat{\xi}_i = \frac{\sum_{\xi} e^{\beta_s m_0 \xi}}{2 \cosh(\beta_s m_0)} \int_{-\infty}^{\infty} Dx \xi \operatorname{sgn}(Jm + \tau h x + \tau_0 h \xi) \quad (17)$$

where we defined the Gaussian integral measure $Dx \equiv dx e^{-x^2/2}/\sqrt{2\pi}$. Equation (15) determines the macroscopic properties of the original image as a snapshot from the Boltzmann-Gibbs distribution at temperature $T_s (\equiv \beta_s^{-1})$. From statistical mechanical point of view, m_0 corresponds to the magnetization of the spin system as an original image $\{\xi\}$. For a specific value of T_s , we obtain m_0 by solving Eq. (15). Substituting T_s , m_0 , τ_0 and τ into Eq. (16), we have the magnetization m for the restored image system $\{\sigma\}$ as a function of $T_m (\equiv J^{-1})$ and h . Then, we substitute $m(T_m, h)$ into the expression of M , and find the hyper-parameter dependence of the overlap explicitly. In FIG. 1, we plot the overlap M as a function of $1/J (\equiv T_m)$. We set $\tau = \tau_0 = 1$ ($\beta_{\tau} = \tau_0/\tau^2 = 1$) and the temperature of the original image is chosen as $T_s = 0.9$. The overlap for the two cases of the field h , namely, $h = \beta_{\tau} T_s J = \tau_0 T_s J / \tau^2 = 0.9J \equiv h_{\text{opt}}$ (a) and $h = 1$ (b), are shown. We should notice that the MAP estimate is obtained in the limit of $T_m \rightarrow 0$ on the condition that the ratio h/J is a constant. Therefore, the overlap for the MAP estimate depends on the ratio h/J and takes its maximum when we set $h/J = \beta_{\tau} T_s = 0.9$ (see FIG. 1 (a)). From these two figures, we see that the overlap takes its maximum at $T_m = T_s = 0.9$ and $h = \beta_{\tau} = \tau_0/\tau^2 = 1$. In the next section, we focus our attention on the dynamics of the MPM estimation.

III. DYNAMICS OF IMAGE RESTORATION

In the previous section, we showed the performance of the MPM estimation by statistical mechanics. However, in that calculations, we assumed that the system reaches its equilibrium state. In other words, each state $\{\sigma\}$ obeys the Boltzmann-Gibbs distribution $\sim e^{-\mathcal{H}(\{\sigma\})}$. When we need to generate the distribution $\sim e^{-\mathcal{H}(\{\sigma\})}$ in order to calculate the MPM estimate $\text{sgn}(\langle \sigma_i \rangle_{J,h})$, we usually use the MCMC method and simulate the equilibrium states artificially on computer. Therefore, it is important to study how the system relaxes to its equilibrium state and decide the behavior of the time evolution of the quantities analytically. As long as we know, there is no research to deal with the behavior of the relaxation or the dynamics of image restoration analytically. In this section, for the infinite range MRF model, we derive the differential equations with respect to the macroscopic order parameters of the restored image system from the microscopic Master equation.

First of all, we should remember that the transition rate $w_k(\{\sigma\})$ from the state $\{\sigma\} \equiv (\sigma_1, \sigma_2, \dots, \sigma_k, \dots, \sigma_N)$ to $\{\sigma\}' \equiv (\sigma_1, \sigma_2, \dots, -\sigma_k, \dots, \sigma_N)$ leads to

$$w_k(\{\sigma\}) = \frac{1}{2} [1 - \sigma_k \tanh[h_k(\{\sigma\})]], \quad h_k(\{\sigma\}) = \frac{J}{N} \sum_j \sigma_j + h\tau_k \quad (18)$$

in the context of the Glauber dynamics of the MCMC method. It is important for us to bear in mind that the Hamiltonian $\mathcal{H}(\{\sigma\})$ for the system is rewritten in terms of $h_k(\{\sigma\})$ as

$$\mathcal{H}(\{\sigma\}) = - \sum_k h_k(\{\sigma\}) \sigma_k. \quad (19)$$

Then, the probability $p_t(\{\sigma\})$ that the system visits the state $\{\sigma\}$ at time t obeys the following Master equation

$$\frac{dp_t(\{\sigma\})}{dt} = \sum_{k=1}^N [p_t(F_k(\{\sigma\}))w_k(F_k(\{\sigma\})) - p_t(\{\sigma\})w_k(\{\sigma\})] \quad (20)$$

where we defined single spin flip operator F_k as

$$F_k(\{\sigma\}) = (\sigma_1, \sigma_2, \dots, -\sigma_k, \dots, \sigma_N). \quad (21)$$

Distribution $P_t(m, a)$, which is a probability that the system has the following two macroscopic order parameters

$$m(\{\sigma\}) \equiv \frac{1}{N} \sum_i \sigma_i, \quad a(\{\sigma\}) \equiv \frac{1}{N} \sum_i \tau_i \sigma_i \quad (22)$$

at time t , is written in terms of the distribution $p_t(\{\sigma\})$ of the microscopic state as

$$P_t(m, a) = \sum_{\sigma} p_t(\{\sigma\}) \delta(m - m(\{\sigma\})) \delta(a - a(\{\sigma\})) \quad (23)$$

where $\delta(\dots)$ is the delta function. Taking the derivative of $P_t(m, a)$ w.r.t. t and substituting Eq. (20) into this expression, and making a Taylor expansion in power of $2\tau_i\sigma_i/N$ (so-called *Kramers-Moyal expansion*), we obtain

$$\begin{aligned} \frac{dP_t(m, a)}{dt} &= \frac{\partial}{\partial m} P_t(m, a) \left\{ m - \frac{\sum_{\xi} e^{\beta_s m_0 \xi}}{2 \cosh(\beta_s m_0)} \int_{-\infty}^{\infty} Dx \tanh(Jm + h\tau x + h\tau_0 \xi) \right\} \\ &+ \frac{\partial}{\partial a} \left\{ a - \frac{\sum_{\xi} e^{\beta_s m_0 \xi}}{2 \cosh(\beta_s m_0)} \int_{-\infty}^{\infty} Dx (\tau x + \tau_0 \xi) \tanh(Jm + h\tau x + h\tau_0 \xi) \right\} + \mathcal{O}(N^{-1}). \end{aligned} \quad (24)$$

Thus, we derived the time evolution of the distribution for the macroscopic quantities from the microscopic Master equation Eq. (20). Finally, we construct the differential equations w.r.t. the macroscopic quantities m and a . Substituting the form of the distribution

$$P_t(m) = \delta(m - m(t)) \delta(a - a(t)) \quad (25)$$

into Eq. (24), and calculating some integrals, we obtain

$$\frac{dm}{dt} = -m + \frac{\sum_{\xi} e^{\beta_s m_0 \xi}}{2 \cosh(\beta_s m_0)} \int_{-\infty}^{\infty} Dx \tanh(Jm + h\tau x + h\tau_0 \xi) \quad (26)$$

$$\frac{da}{dt} = -a + \frac{\sum_{\xi} e^{\beta_s m_0 \xi}}{2 \cosh(\beta_s m_0)} \int_{-\infty}^{\infty} Dx (\tau x + \tau_0 \xi) \tanh(Jm + h\tau x + h\tau_0 \xi). \quad (27)$$

These two equations describe the relaxation of the system to its equilibrium state. We should notice that order parameter a is a slave variable in the sense that the order parameter m relaxes independently, whereas the relaxation of a depends on m . Therefore, the

behavior of a is completely determined by m . For this reason, from now on, we disregard Eq. (27).

It is easy to see that in the limit of $t \rightarrow \infty$ and $dm/dt = 0$, the equation of state (16) by the static calculation is recovered. As the overlap M is written in terms of m [see Eq. (17)], the time evolution of the overlap is obtained by substituting the time evolution of the magnetization $m(t)$ into the expression of M . Using the same technique as the procedure to derive the differential equation with respect to m , the differential equation for the magnetization of the prior system, $P(\{\sigma\}) = \exp(J \sum_{ij} \sigma_i \sigma_j) / \sum_{\sigma} \exp(J \sum_{ij} \sigma_i \sigma_j)$, is obtained as

$$\frac{dm_1}{dt} = -m_1 + \tanh(m_1 J). \quad (28)$$

Although in these equations we regard the hyper-parameters J and h as constant variables, one should treat them as time dependent parameters, that is, $J(t)$ and $h(t)$. Of course, the details of the time dependence of $J(t)$ and $h(t)$ depend on the method of hyper-parameter estimations. We should mention that the dynamics of gray-scale image restoration for fixed hyper-parameters was investigated by one of the authors [4]. In the next section, we investigate the properties of hyper-parameter estimation as a dynamical process of $J(t)$ and $h(t)$.

IV. HYPER-PARAMETER ESTIMATION

In the previous two sections, we investigated both static and dynamical properties of image restoration. From those results, we saw that the hyper-parameter dependence of the overlap explicitly. However, in the practical situations, we do not mention about the optimal value of the hyper-parameters before hand. Therefore, we need to determine the optimal value from only information about the degraded image $\{\tau\}$.

About ten years ago, Iba [13] studied the performance of the method of the MML with assistance of the MCMC method for the same problem as ours. However, as he mentioned

in his paper, the results are not enough to make its performance clear due to the difficulties of simulating the equilibrium state within reliable precision. With this fact in mind, in this section, we calculate the marginal likelihood as a function of hyper-parameters and magnetization m analytically. From the marginal likelihood, we derive the Boltzmann machine-type learning equations and investigate the behavior quantitatively.

A. Maximization of marginal likelihood method

In statistics, several authors [1,8,12] used the maximum marginal likelihood (MML) method to infer the hyper-parameter appearing in the posterior. In the context of image restoration we treat here, the marginal likelihood (logarithm of marginal likelihood) is given by

$$\begin{aligned}
-K(J, h) &\equiv \log \sum_{\sigma} P(\{\tau\}|\{\sigma\})P(\{\sigma\}) \\
&= \log \left(\sum_{\sigma} e^{J \sum_{ij} \sigma_i \sigma_j + h \sum_i \tau_i \sigma_i} \right) - \log Z_{\Pi} - \log Z_L.
\end{aligned} \tag{29}$$

Usually, we attempt to maximize the marginal likelihood by using gradient descent w.r.t. J and h . This result leads to the following Boltzmann machine-type learning equations

$$c_J \frac{dJ}{dt} = -\frac{\partial K(J, h)}{\partial J} = \frac{\sum_{\sigma} (\sum_{ij} \sigma_i \sigma_j) e^{J \sum_{ij} \sigma_i \sigma_j + h \sum_i \tau_i \sigma_i}}{\sum_{\sigma} e^{J \sum_{ij} \sigma_i \sigma_j + h \sum_i \tau_i \sigma_i}} - \frac{\sum_{\sigma} (\sum_{ij} \sigma_i \sigma_j) e^{J \sum_{ij} \sigma_i \sigma_j}}{\sum_{\sigma} e^{J \sum_{ij} \sigma_i \sigma_j}} \tag{30}$$

$$c_h \frac{dh}{dt} = -\frac{\partial K(J, h)}{\partial h} = \frac{\sum_{\sigma} (\sum_i \tau_i \sigma_i) e^{J \sum_{ij} \sigma_i \sigma_j + h \sum_i \tau_i \sigma_i}}{\sum_{\sigma} e^{J \sum_{ij} \sigma_i \sigma_j + h \sum_i \tau_i \sigma_i}} - \frac{\partial \log Z_L}{\partial h} \tag{31}$$

where c_J and c_h are relaxation times and in this paper we fix these values as $c_J = c_h = 1$. Thus, by solving these two equations, we maximize the marginal likelihood $-K(J, h)$ and obtain an appropriate solution as a fixed point of the equations. However, these two equations contain the expectations of the quantities $\sum_{ij} \sigma_i \sigma_j$ and $\sum_i \tau_i \sigma_i$ over the posterior and the prior distributions. When we solve Eqs. (30), (31) numerically, we should calculate these expectations at each time step of the Euler method. Iba [13] carried out the MCMC method to calculate the expectations and evaluated the time dependence

of the hyper-parameters J and h numerically although the precision of the simulations is not reliable. In this subsection, we use the infinite range MRF model and derive the learning equations (30),(31) analytically.

Our interest is averaged performance of the MML method, instead of the performance for a specific choice of the original image and the degraded process, the quantity we should first evaluate is the following averaged marginal likelihood;

$$- [K(J, h)]_{\{\xi, \tau\}} = \left[\log \sum_{\sigma} e^{\frac{J}{N} \sum_{ij} \sigma_{ij} \sigma_i \sigma_j + h \sum_i \tau_i \sigma_i} \right]_{\{\xi, \tau\}} - \left[\log \sum_{\sigma} e^{\frac{J}{N} \sum_{ij} \sigma_i \sigma_j} \right]_{\{\xi, \tau\}} - [\log Z_L]_{\{\xi, \tau\}} \quad (32)$$

where the bracket $[\dots]_{\{\xi, \tau\}}$ means the average over the distribution $P(\{\tau\}|\{\xi\})P(\{\xi\})$. In general, it is hard to carry out this kind of the average, namely, $[\log Z]_{\{\xi, \tau\}}$ ($Z \equiv \sum_{\sigma} \exp((J/N) \sum_{ij} \sigma_i \sigma_j + h \sum_i \tau_i \sigma_i)$, for example). Then, we replace the average of $\log Z$ with the average of the n -th moment of Z , that is, Z^n by using

$$[\log Z]_{\{\xi, \tau\}} = \lim_{n \rightarrow 0} \frac{[Z^n]_{\{\xi, \tau\}} - 1}{n}. \quad (33)$$

This trick is referred to as *replica method* [14]. By the assistant of the replica method, we obtain the averaged marginal likelihood per pixel as

$$- \frac{[K]_{\{\xi, \tau\}}}{N} = -\frac{J}{2} m^2 + \frac{\sum_{\xi} e^{\beta_s m_0 \xi}}{2 \cosh(\beta_s m_0)} \int_{-\infty}^{\infty} Dx \log 2 \cosh(Jm + h\tau x + h\tau_0 \xi) + \frac{J}{2} m_1^2 - \log 2 \cosh(m_1 J) + \frac{\tau_0}{2\tau^2} - \frac{\tau^2 h^2}{2} \equiv -K \quad (34)$$

where m and m_1 are magnetizations of the spin systems described by the posterior and the prior, respectively. In FIG. 2, we plot the $-K$ as a function of J and h . In this figure, we see that the averaged marginal likelihood takes its maximum when we choose the hyper-parameters so as to be identical to the true values. This fact is easily checked by the following inequality

$$[K(\beta_s, \beta_{\tau})]_{\{\xi, \tau\}} - [K(J, h)]_{\{\xi, \tau\}} = \sum_{\xi, \tau} P_{\beta_{\tau}}(\{\tau\}|\{\xi\}) P_{\beta_s}(\{\xi\}) \log \sum_{\sigma} P_{\beta_{\tau}}(\{\tau\}|\{\sigma\}) P_{\beta_s}(\{\sigma\})$$

$$\begin{aligned}
& - \sum_{\xi, \tau} P_{\beta_\tau}(\{\tau\}|\{\xi\}) P_{\beta_s}(\{\xi\}) \log \sum_{\sigma} P_h(\{\tau\}|\{\sigma\}) P_J(\{\sigma\}) \\
& = \sum_{\tau} P_{\beta_s, \beta_\tau}(\{\tau\}) \log(P_{J,h}(\{\tau\})/P_{\beta_s, \beta_\tau}(\{\tau\})) \geq 0 \quad (35)
\end{aligned}$$

where we used the non-negativity of the *Kullback-Libeler information* and we defined

$$P_X(\{\tau\}|\{\sigma\}) \equiv \frac{\exp(X \sum_i \tau_i \xi_i)}{\sum_{\sigma} \exp(X \sum_i \tau_i \xi_i)} \quad (36)$$

$$P_X(\{\xi\}) \equiv \frac{\exp(X \sum_{ij} \xi_i \xi_j)}{\sum_{\sigma} \exp(X \sum_{ij} \xi_i \xi_j)}, \quad P_{X,Y}(\{\tau\}) \equiv \sum_{\xi} P_X(\{\tau\}|\{\xi\}) P_Y(\{\xi\}). \quad (37)$$

Thus, we confirm that our model is not against this general inequality. We should mention that the present authors also studied the hyper-parameter estimation by using another kind of the exactly solvable MRF model, namely, so-called *Gaussian model* [15].

For this marginal likelihood (32), the learning equations are obtained by the following gradient descent

$$c_J \frac{dJ}{dt} = - \left[\frac{\partial K(J, h)}{\partial J} \right]_{\{\xi, \tau\}}, \quad c_h \frac{\partial h}{\partial t} = - \left[\frac{\partial K(J, h)}{\partial h} \right]_{\{\xi, \tau\}}. \quad (38)$$

The right hand side of the above equations are also evaluated by the replica method. After some complicated calculations, we obtain

$$\begin{aligned}
c_J \frac{dJ}{dt} &= -\frac{m^2}{2} + m \frac{\sum_{\xi} e^{\beta_s m_0 \xi}}{2 \cosh(\beta_s m_0)} \int_{-\infty}^{\infty} Dx \tanh(Jm + h\tau x + h\tau_0 \xi) \\
&\quad + \frac{m_1^2}{2} - m_1 \tanh(m_1 J) \quad (39)
\end{aligned}$$

$$c_h \frac{dJ}{dt} = \frac{\sum_{\xi} e^{\beta_s m_0 \xi}}{2 \cosh(\beta_s m_0)} \int_{-\infty}^{\infty} Dx (\tau x + \tau_0 \xi) \tanh(Jm + h\tau x + h\tau_0 \xi) - \tau^2 h \quad (40)$$

where we should remember that m and m_1 obey

$$\frac{dm}{dt} = -m + \frac{\sum_{\xi} e^{\beta_s m_0 \xi}}{2 \cosh(\beta_s m_0)} \int_{-\infty}^{\infty} Dx \tanh(Jm + h\tau x + h\tau_0 \xi) \quad (41)$$

$$\frac{dm_1}{dt} = -m_1 + \tanh(m_1 J) \quad (42)$$

as we saw in Eqs. (26) and (28). By solving these coupled equations, we find the behavior of the hyper-parameters $J(t)$, $h(t)$ and the relaxation processes of the systems, namely,

$m(t), m_1(t)$. In FIG. 3, we plot the time dependence of the hyper-parameter J . From this figure, we see that the final state is optimal value $J = 1/0.9 \simeq 1.1$ and this convergent point does not depend on the choice of the initial state. In FIG. 5, we plot the flow of hyper-parameter $J-h$. From this figure, we find that each flow does not take the shortest path to the solution and goes a long way around the solution.

B. EM algorithm

In the previous section, we investigated the process of the MML method by gradient decent as a dynamics. In this section, we analyze the performance of the *EM algorithm* [9] as another candidate to maximize the marginal likelihood indirectly. In the EM algorithm, we first average the complete data log-likelihood function

$$\begin{aligned} \log P(\{\tau\}|\{\sigma\})P(\{\sigma\}) &= J \sum_{ij} \sigma_i \sigma_j + h \sum_i \tau_i \sigma_i - \log \sum_{\sigma} \exp(J \sum_{ij} \sigma_i \sigma_j / N) \\ &\quad + \frac{N\tau_0}{2\tau^2} - \frac{N\tau^2 h^2}{2} \end{aligned} \quad (43)$$

over the time dependent posterior

$$P_t(\{\sigma\}|\{\tau\}) = \frac{e^{J_t \sum_{ij} \sigma_i \sigma_j + h_t \sum_i \tau_i \sigma_i}}{\sum_{\sigma} e^{J_t \sum_{ij} \sigma_i \sigma_j + h_t \sum_i \tau_i \sigma_i}}. \quad (44)$$

This average is referred to as *Q-function* and leads to

$$\begin{aligned} Q(J, h | J_t, h_t) &= \left[\sum_{\sigma} P_t(\{\sigma\}|\{\tau\}) \log P(\{\tau\}|\{\sigma\})P(\{\sigma\}) \right]_{\{\xi, \tau\}} \\ &= J \left[\frac{\sum_{\sigma} (\sum_{ij} \sigma_i \sigma_j) e^{J_t \sum_{ij} \sigma_i \sigma_j + h_t \sum_i \tau_i \sigma_i}}{\sum_{\sigma} e^{J_t \sum_{ij} \sigma_i \sigma_j + h_t \sum_i \tau_i \sigma_i}} \right]_{\{\xi, \tau\}} \\ &\quad + h \left[\frac{\sum_{\sigma} (\sum_i \tau_i \sigma_i) e^{J_t \sum_{ij} \sigma_i \sigma_j + h_t \sum_i \tau_i \sigma_i}}{\sum_{\sigma} e^{J_t \sum_{ij} \sigma_i \sigma_j + h_t \sum_i \tau_i \sigma_i}} \right]_{\{\xi, \tau\}} \\ &\quad - \log \sum_{\sigma} \exp(J \sum_{ij} \sigma_i \sigma_j / N) + \frac{N\tau_0^2}{2\tau^2} - \frac{N\tau^2 h^2}{2}. \end{aligned} \quad (45)$$

Then, EM algorithm is summarized as follows.

- Step 1.

Set the initial values of the hyper-parameters J_0 , h_0 and $t \leftarrow 0$.

- Step 2.

Iterate the following E and M steps until appropriate convergence condition is satisfied.

– E step : Calculate $Q(J, h|J_t, h_t)$.

– M step :

$$J_{t+1} = \operatorname{argmax}_J Q(J, h|J_t, h_t)$$

$$h_{t+1} = \operatorname{argmax}_h Q(J, h|J_t, h_t)$$

and $t \leftarrow t + 1$.

For our infinite range MRF model, the average $[\cdot \cdot]_{\{\xi, \tau\}}$ is calculated by using replica method and we obtain

$$\begin{aligned} \frac{Q(J, h|J_t, h_t)}{N} &= -\frac{Jm(t)^2}{2} + \frac{Jm(t) \sum_{\xi} e^{\beta_s m_0 \xi}}{2 \cosh(\beta_s m_0)} \int_{-\infty}^{\infty} Dx \tanh(J_t m(t) + h_t \tau x + h_t \tau_0 \xi) \\ &+ \frac{h \sum_{\xi} e^{\beta_s m_0 \xi}}{2 \cosh(\beta_s m_0)} \int_{-\infty}^{\infty} Dx (\tau x + \tau_0 \xi) \tanh(J_t m(t) + h_t \tau x + h_t \tau_0 \xi) \\ &+ \frac{J}{2} m_1(t)^2 - \log 2 \cosh(m_1(t) J) + \frac{\tau_0^2}{2\tau^2} - \frac{\tau^2 h^2}{2}. \end{aligned} \quad (46)$$

The parameters of the next time step, namely, J_{t+1} and h_{t+1} are given by the solution of the equations $\partial Q / \partial J = 0$ and $\partial Q / \partial h = 0$. These two equations are explicitly lead to the following non-linear maps

$$\begin{aligned} J_{t+1} &= \frac{1}{m(t)} \tanh^{-1} \left[-\frac{\{m(t)^2 - m_1(t)^2\}^2}{2m_1(t)} \right. \\ &\left. + \frac{m(t) \sum_{\xi} e^{\beta_s m_0 \xi}}{2m_1(t) \cosh(\beta_s m_0)} \int_{-\infty}^{\infty} Dx \tanh(J_t m(t) + h_t \tau x + h_t \tau \xi) \right] \end{aligned} \quad (47)$$

$$h_{t+1} = \frac{\sum_{\xi} e^{\beta_s m_0 \xi}}{2\tau^2 \cosh(\beta_s m_0)} \int_{-\infty}^{\infty} Dx (\tau x + \tau_0 \xi) \tanh(J_t m(t) + h_t \tau x + h_t \tau_0 \xi). \quad (48)$$

In the above expressions, $m(t)$ and $m_1(t)$ are time dependent magnetizations for the systems described by the posterior $P(\{\sigma\}|\{\tau\})$ and the prior $P(\{\sigma\})$, respectively. By using mean-field approximation, we obtain the following non-linear maps w.r.t. $m(t)$ and $m_1(t)$

$$m(t+1) = \frac{\sum_{\xi} e^{\beta_s m_0 \xi}}{2 \cosh(\beta_s m_0)} \int_{-\infty}^{\infty} Dx \tanh(J_t m(t) + h_t \tau x + h_t \tau_0 \xi) \quad (49)$$

$$m_1(t+1) = \tanh(J_t m_1(t)). \quad (50)$$

By solving these non-linear maps Eqs. (47)-(50), we obtain the time dependence of the hyper-parameters J_t, h_t and the magnetizations $m(t), m_1(t)$. We plot the results in FIG. 5 (right) and FIG. 6. From these figures, we see that both the MML method by gradient descent and the EM algorithm obtain the optimal hyper-parameters $(J_*, h_*) = (1.1, 1)$, however, the EM algorithm shows faster convergence than the MML by gradient descent and the flows in the hyper-parameter space (J, h) are shorter than the MML by gradient descent. From the posterior distribution appearing in the Q-function (45), we see that the performance of the EM algorithm highly depends on the initial choice of the hyper-parameters, J_0 and h_0 . Therefore, for the systems which have lots of local minima, the final solution is sensitive to the initial condition on the hyper-parameters. For our model system in image restoration (the infinite range random field Ising model), there is no local minima in the marginal likelihood function. As the result, the final state of the EM algorithm was independent of the initial conditions.

V. SUMMARY

In this paper, we investigated dynamical properties of image restoration by using statistical mechanics. We introduced an infinite range MRF model and solved it analytically. We derived the differential equations with respect to the macroscopic order parameters from the microscopic Master equation. We also studied the dynamics of hyper-parameter estimation in the context of the maximum marginal likelihood by gradient descent and the

EM algorithm. For the MML method by gradient descent, the Boltzmann machine-type learning equations were evaluated analytically by the replica method. On the other hand, the EM algorithm led to the non-linear maps and these maps were also evaluated analytically. We compared these two methods and found that for both methods, we obtain the optimal hyper-parameters, however, the speed of convergence for the EM algorithm is faster than that of the MML method by gradient descent. In addition, the paths to the solution in hyper-parameter space by the EM algorithm are shorter than those of the MML by gradient descent. Thus, in this paper, we could compare two different methods to estimate the hyper-parameters without any computer simulations. Our analytical treatments are applicable to the studies of the performance for the other method including the DAEM algorithm [16,17]. Of course, besides the problems of image restorations, our approach is useful for the other problem, for example, problems of learning by Bayesian neural networks, time series predictions or density estimation problem [18].

We thank Hidetoshi Nishimori, Masato Okada, Yukito Iba and David Saad for fruitful discussion. Our special thanks are due to Toshiyuki Tanaka for useful discussion and comments.

FIGURES

FIG. 1. $1/J(\equiv T_m)$ dependence of the overlap M . Temperature of the original image is $T_s = 0.9$ and the noise level is $\beta_\tau = \tau_0/\tau^2 = 1(\tau_0 = \tau = 1)$. We set the field h as $h = \beta_\tau T_s J = (\tau_0 T_s / \tau^2) J = 0.9J \equiv h_{\text{opt}}$ (a) and $h = 1$ (b). In the limit of $1/J \rightarrow 0$, we obtain the overlap of the MAP estimation. In both cases (a) and (b), overlap M takes its maximum at $T_m = T_s = 0.9$.

FIG. 2. J -dependence of the marginal likelihood $-K$ (upper figure). We set $h = 0.5, 1$ and $h = 1.5$. We see that $-K$ takes its maximum when we choose J, h as $J = 1.1(= 1/T_s)$ and $h = \beta_\tau = 1$. h -dependence of the marginal likelihood $-K$ (lower figure). We set $J = 0.5, 1$ and $J = 2.1$. We see that $-K$ takes its maximum when we choose J, h as $J = 1.1 = (1/T_s)$ and $h = \beta_\tau = 1$.

FIG. 3. From the upper left to the lower right, time dependence of the hyper-parameters J , h and the magnetizations m , m_1 . In each graph, we choose the initial condition (a) $J(0) = 0.45, h(0) = 1, m(0) = m_1(0) = 0.4$, (b) $J(0) = 0.45, h(0) = 0.5, m(0) = m_1(0) = 0.4$, (c) $J(0) = 2.25, h(0) = 1, m(0) = m_1(0) = 0.4$, (d) $J(0) = 2.25, h(0) = 0.5, m(0) = m_1(0) = 0.4$. We set true value of the hyper-parameters $T_s = 0.9, \beta_\tau = 1$

FIG. 4. Time dependence of the overlap M for the case of the MML by gradient descent (upper figure) and the case of the EM algorithm (lower figure). For both cases, we choose the initial condition as (a) $J(0) = 0.45, h(0) = 1, m(0) = m_1(0) = 0.4$, (b) $J(0) = 0.45, h(0) = 0.5, m(0) = m_1(0) = 0.4$, (c) $J(0) = 2.25, h(0) = 1, m(0) = m_1(0) = 0.4$, (d) $J(0) = 2.25, h(0) = 0.5, m(0) = m_1(0) = 0.4$. We set true value of the hyper-parameters $T_s = 0.9, \beta_\tau = 1$. We see that for both cases, the optimal overlap M_{opt} is obtained as a fixed point of the dynamics.

FIG. 5. Flows in the hyper-parameter space (J, h) . We set $J(0) = J_0 = 0.45, h(0) = h_0 = 1$, and $m(0) = m_1(0) = 0.4$ (upper figure) and $J(0) = J_0 = 2.25, h(0) = h_0 = 1$ and $m(0) = m_1(0) = 0.4$ (lower figure). True values of the hyper-parameters are $J_* = 1/T_s = 1.1, h_* = \beta_\tau = 1$. For the case of the gradient descent (GD), the flows go a long way around the solution $(J_*, h_*) = (1.1, 1)$. In order to compare the MML by gradient descent with the EM algorithm, we plot the flows of the EM algorithm in the same figures. We see that the EM takes shorter paths than the MML by gradient descent.

FIG. 6. From the upper left to the lower right, The time dependence of the hyper-parameters J, h and the magnetizations m, m_1 for the EM algorithm. In each graph, we choose the initial condition (a) $J_0 = 0.45, h_0 = 1, m(0) = m_1(0) = 0.4$, (b) $J_0 = 0.45, h_0 = 0.5, m(0) = m_1(0) = 0.4$, (c) $J_0 = 2.25, h_0 = 1, m(0) = m_1(0) = 0.4$, (d) $J_0 = 2.25, h_0 = 0.5, m(0) = m_1(0) = 0.4$. We set true value of the hyper-parameters $T_s = 0.9, \beta_\tau = 1$

REFERENCES

- [1] J. M. Pryce and A. D. Bruce, *J. Phys. A: Math. Gen.* **28** 511 (1995).
- [2] H. Nishimori and K. Y. M. Wong, *Phys. Rev. E* **60** 132 (1999).
- [3] D. M. Carlucci and J. Inoue, *Phys. Rev. E* **60** 2547 (1999).
- [4] J. Inoue and D. M. Carlucci, to appear in *Phys. Rev. E* **64** (2001).
- [5] S. Geman and D. Geman, *IEEE Trans. on Pattern Analysis and Machine Intelligence* **6** 721 (1984).
- [6] J. Marroquin, S. Mitter and T. Poggio, *Journal of the American Statistical Association* **82** 76 (1989).
- [7] K. Tanaka, *Transactions of the Japanese Society for Artificial Intelligence* **16** 246 (2001).
- [8] S. Geman and D. E. McClure, *Bull. Internat. Statist. Inst.* **52** 5 (1987).
- [9] A. P. Dempster, N. M. Laird and D. B. Rubin, *Journal of the Royal Statistics, Series B (methodological)* **39** 1 (1977).
- [10] S. Kirkpatrick, G. D. Gellatt Jr. and M. P. Vecchi, *Science* **220** 671 (1983).
- [11] D. Geiger and F. Girosi, *IEEE Trans. on Pattern Analysis and Machine Intelligence* **13** 401(1991).
- [12] Z. Zhou, R. M. Leahy and J. Qi, *IEEE Trans. Image Processing* **6** 844 (1997).
- [13] Y. Iba, *Proceedings of the Institute of Statistical Mathematics, (in Japanese)*, **39** 1 (1991).
- [14] D. Sherrington and S. Kirkpatrick, *Phys. Rev. Lett.* **35**, 1792(1975).
- [15] K. Tanaka and J. Inoue, Technical report of the Institute of Electronics, Information

and Communication Engineers, (in Japanese), **PRMU2000-125** 41 (2000).

[16] R. L. Streit and T. E. Luginbuhl, *IEEE Trans. Neural Networks* **5** 764 (1994).

[17] N. Ueda and R. Nakano, *Proc. of IEEE Neural Networks for Signal Processing*, 1211 (1994).

[18] N. Barkai and H. Sompolinsky, *Phys. Rev. E* **50** 1766 (1994).

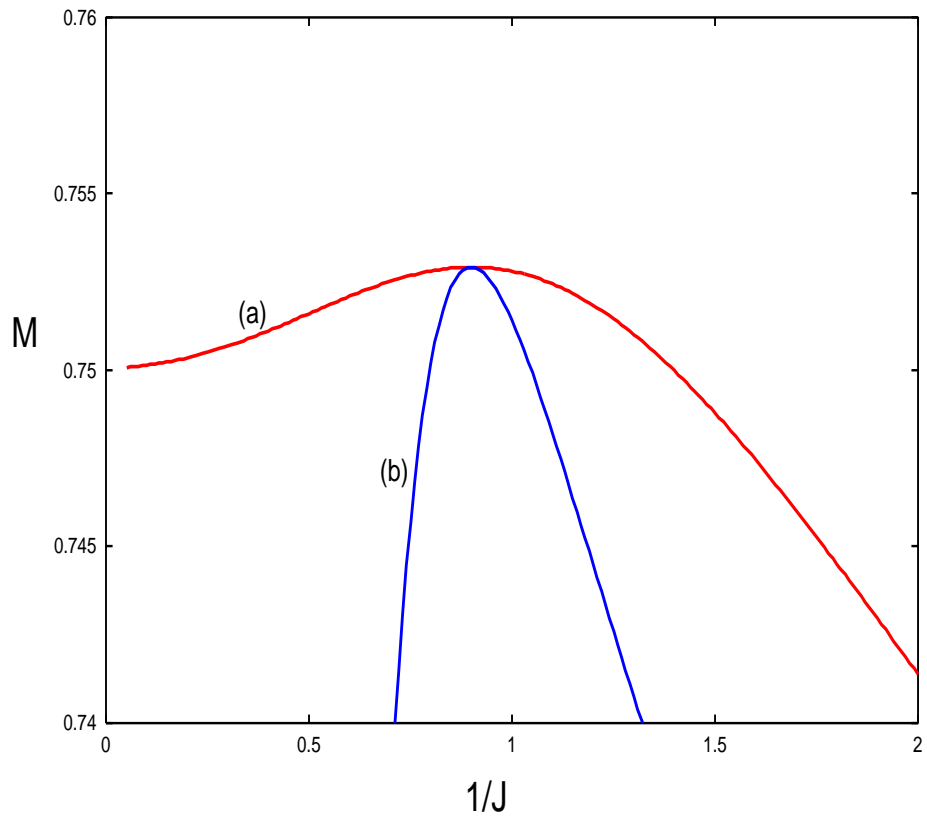


FIG. 1

Inoue and Tanaka

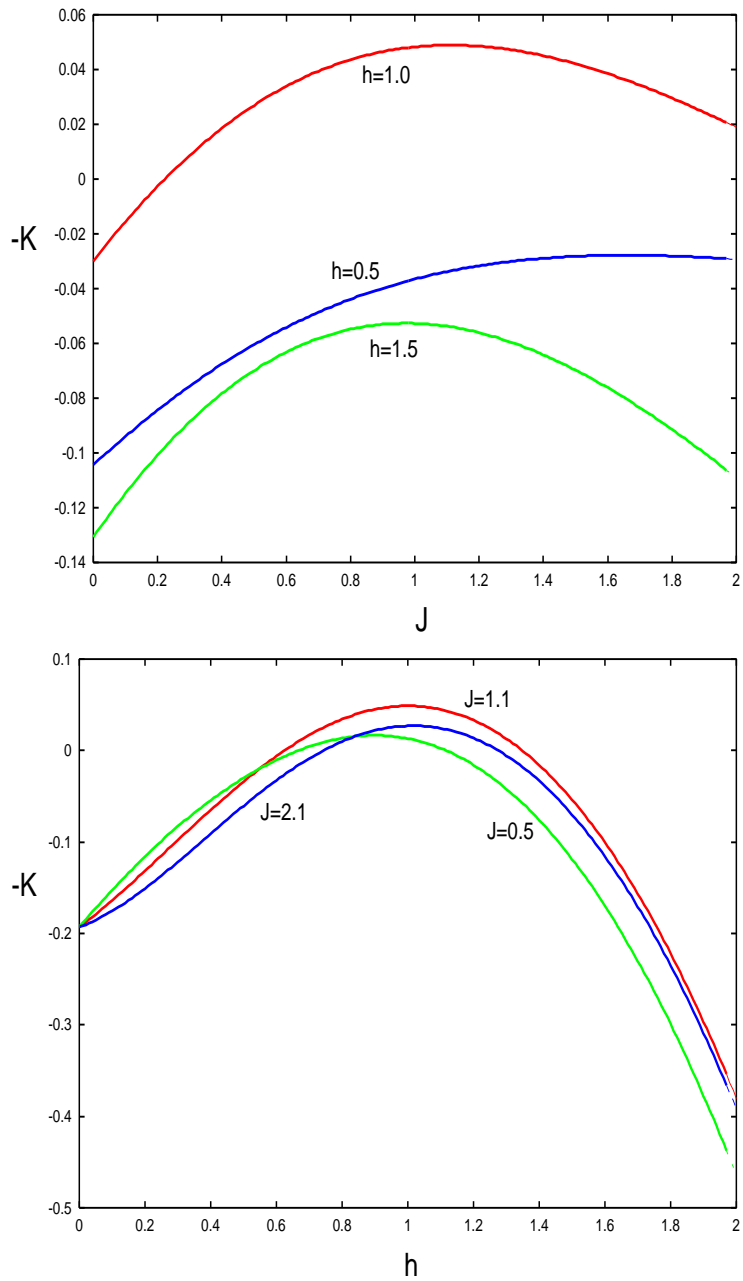


FIG. 2

Inoue and Tanaka

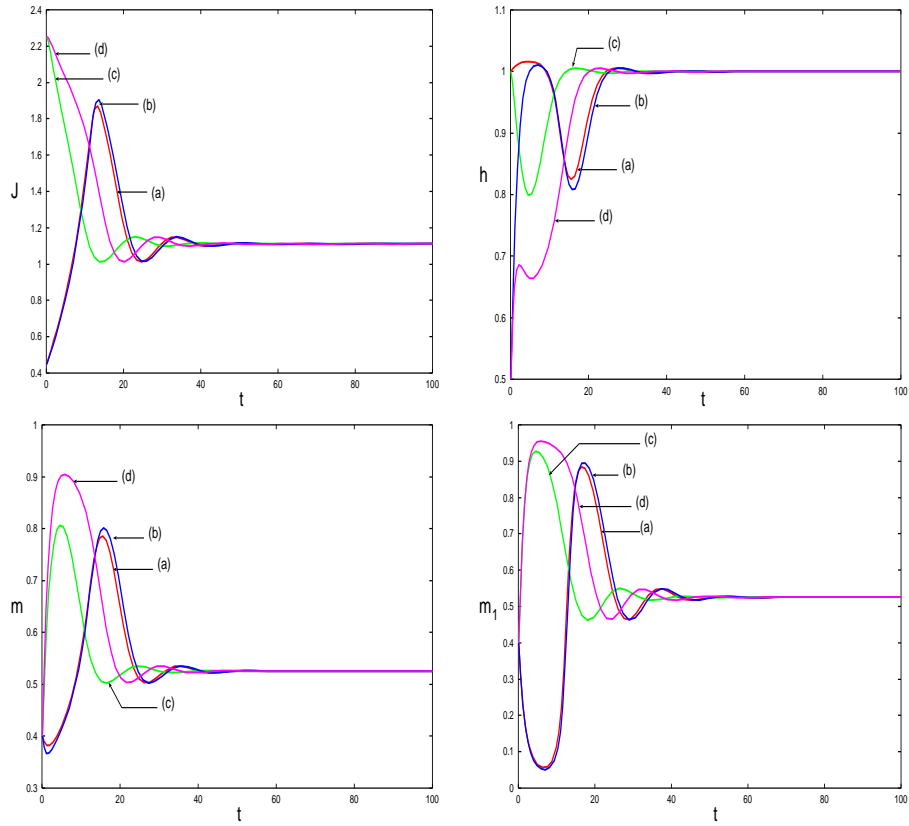


FIG. 3

Inoue and Tanaka

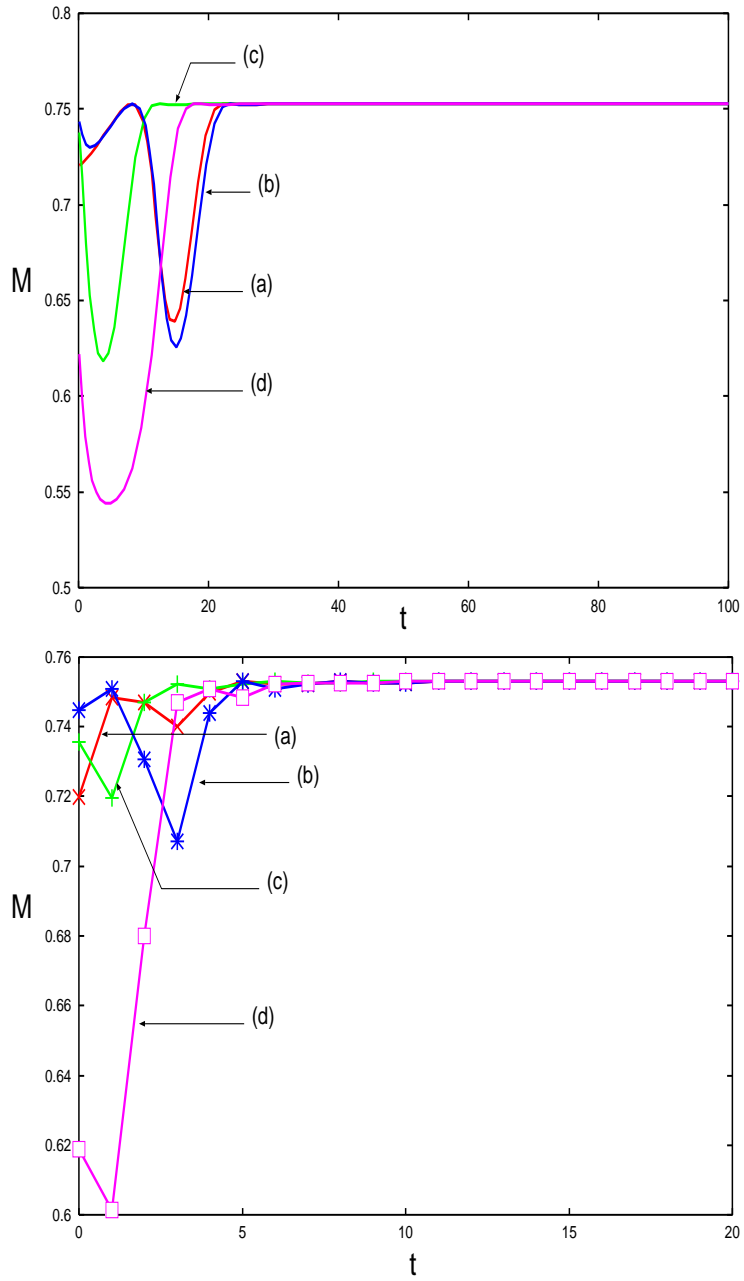


FIG. 4

Inoue and Tanaka

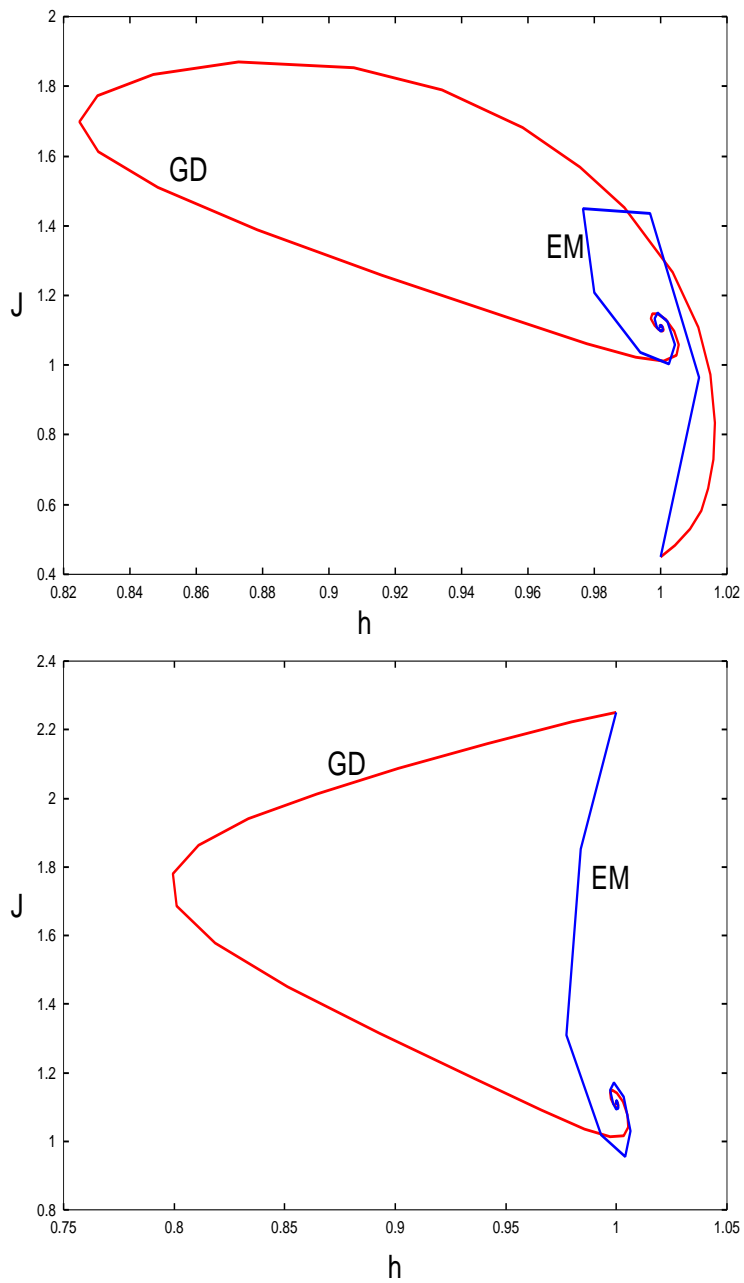


FIG. 5

Inoue and Tanaka

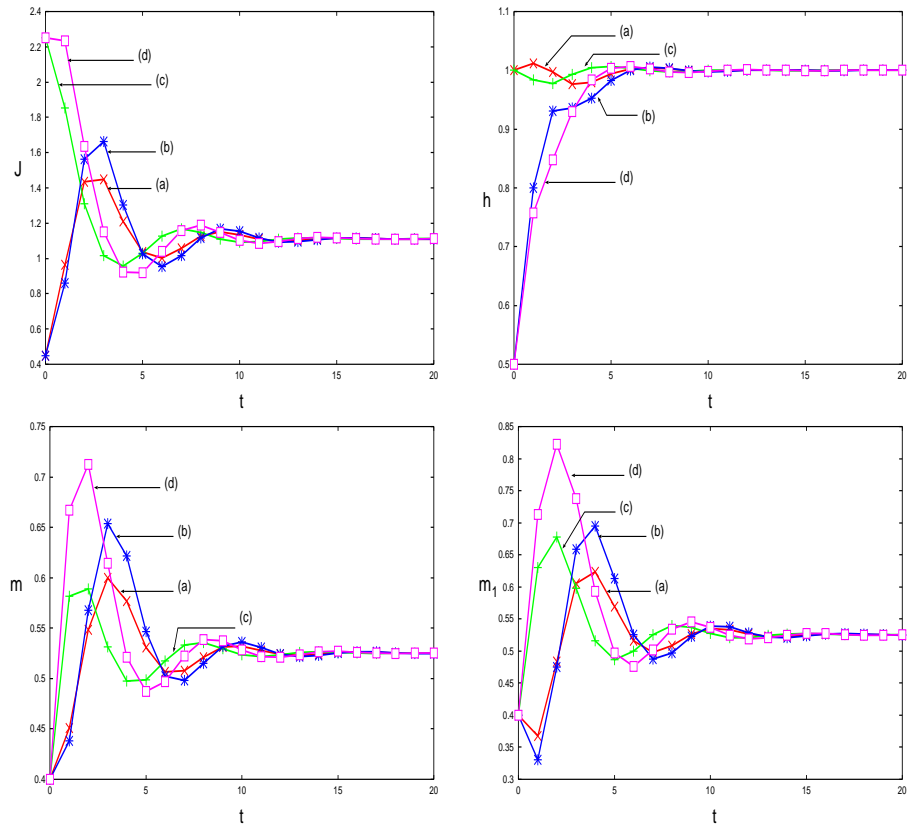


FIG. 6

Inoue and Tanaka